STUDY ON COLLAPSE OF FLEXURE-SHEAR-CRITICAL REINFORCED CONCRETE FRAMES

S. Yavari[1], S.H. Lin[2], K.J. Elwood[3], C.L. Wu[4], S.J. Hwang[5], and J.P. Moehle[6]

[1] *PhD Candidate, Dept. of Civil Engineering, University of British Columbia, Vancouver, Canada*
[2] *M.Sc. Candidate, Dept. of Civil Engineering, National Taiwan University, Taipei, Taiwan*
[3] *Associate Professor, Dept. of Civil Engineering, University of British Columbia, Vancouver, Canada*
[4] *Associate Research Fellow, National Center for Research on Earthquake Engineering, Taipei, Taiwan*
[5] *Professor, Dept. of Civil Engineering, National Taiwan University, Taipei, Taiwan*
[6] *Professor, Dept. of Civil and Environmental Engineering, University of California, Berkeley, USA*

Email: syavari@civil.ubc.ca

ABSTRACT:

In order to observe the interaction of structural elements at the onset of collapse, four frame specimens are planned to be tested at the National Center for Research on Earthquake Engineering (NCREE) in Taiwan in 2008. Each specimen consists of a half-scale model of a two-bay and two-story reinforced concrete frame. The specimens are tested under high and low gravity loads to investigate the influence of axial loads on the collapse vulnerability of the structures. These tests will also be employed to study the interaction of the beams, columns and joints as collapse is initiated. The current paper presents the blind prediction of the behavior of the frame specimens by simulating the shaking table tests using existing analytical models. Empirical capacity models were used to predict the hysteretic response of shear-critical reinforced concrete columns under gravity and seismic loading. In particular, the shear failure and axial load collapse of these columns were closely examined. The finite element program OpenSEES, developed by the Pacific Earthquake Engineering Research Center, was employed to conduct the analyses. Following the shaking table tests, the results of the blind prediction, presented in this paper, will be compared to the experimental data. This comparison will illustrate the limitations, weaknesses, and strengths of current analytical models. Such studies will lead to a better prediction of the behavior of existing reinforced concrete structures, and consequently, more cost-effective retrofit strategies.

KEYWORDS: collapse, shaking table tests, non-ductile concrete frames, concrete columns, concrete beam-column joints, shear and axial failure.

1. INTRODUCTION

Observations of damage after earthquakes and experimental research have indicated that existing building columns with light and inadequately detailed transverse reinforcement are vulnerable to shear failure during ground shaking. Shear failure causes reduction in building lateral strength, lower axial load carrying capacity, and a change in the inelastic deformation mechanism of frames, potentially leading to collapse of the building. Modern seismic design codes around the world emphasize the need for adequate transverse reinforcement to provide columns with toughness and ductility during seismic shaking; however, a large number of reinforced concrete structures have been constructed prior to introduction of modern seismic provisions. The vast number of older structures in earthquake-prone areas around the globe, coupled with the overwhelming proportion of such structures that would require retrofit if evaluated according to current assessment procedures (e.g. ASCE 2008), is hindering worldwide mitigation efforts.

In contrast with the prevalence collapse predictions based on current assessment procedures, post-earthquake reconnaissance studies show a relatively low rate of collapse amongst older non-seismically detailed concrete structures even in major earthquakes (Otani 1999). These observations suggest that current practices for assessing collapse are conservative and more refined engineering tools are required to identify the critical buildings that are most collapse-prone so that resources can be focused on the seismic mitigation of such buildings. Through a better understanding of mechanisms that cause collapse, improved engineering tools may be developed for use by practicing engineers to assess the collapse vulnerability of poor detailed reinforced concrete frame structures. This has been the aim of several recent studies and continues to be a high priority for improving seismic safety worldwide. The main objective of this study is to investigate, both experimentally and analytically, the seismic collapse behavior of non-seismically detailed reinforced concrete frames. Particularly, this study tries to investigate structural framing effects on column shear and axial failures, and conversely, the effects of column failures on frame system collapse vulnerability. Understanding these interactions is essential in assessing the collapse vulnerability of structures. Engineering models for the shear and axial load response of columns will be validated by the results from the proposed shaking table tests.

2. SIGNIFICANCE OF THE RESEACH

Collapse of a reinforced concrete frame during an earthquake can be caused by failure of beams, columns, or beam-column joints. Older gravity-based design methods resulted in a system with weak columns and strong beams, and therefore, most building frames designed using such methods are expected to experience failure of columns or joints. To date, there have been relatively few tests on lightly confined reinforced concrete frame systems in the literature and rarely conducted dynamically to collapse. None of these tests investigated the effects of high axial load on the failure of non-ductile columns. In an attempt to fill the gaps in knowledge, this study involves dynamic testing to collapse of four two-dimensional, two-bay, two-story, and half-scale reinforced concrete frames. Each frame contains non-seismically detailed columns whose proportions and reinforcement details allow them to yield in flexure prior to shear strength degradation and ultimately reach axial collapse (these columns are commonly referred to as flexure-shear-critical columns). The influence of non-confined joints on the collapse behavior of the frame will also be investigated. Figure 1 describes the four shaking table specimens. Comparison of the results from MCFS and HCFS will reveal the influence of axial load on shear and axial behavior of flexure-shear-critical columns, while observations from MUF and MUFS will demonstrate the effects of unconfined joints on overall behavior of the frame near the point of collapse and sequence of failure in the elements. Details of the specimens are described in the following section.

Specimen MCFS: **M**oderate Axial Load **C**onfined Joints **F**lexure-**S**hear Columns	**Specimen HCFS:** **H**igh Axial Load **C**onfined Joints **F**lexure-**S**hear Columns
Specimen MUFS: **M**oderate Axial Load **U**nconfined Joints **F**lexure-**S**hear Columns	**Specimen MUF:** **M**oderate Axial Load **U**nconfined Joints **F**lexure Columns

Figure 1: Description of shaking table specimens

3. SPECIMENS AND TEST SETUP

3.1. Specimen Design

Four half-scale frames with two stories and three flexure-shear-critical columns were designed to be tested on the shaking table at the National Center for Research in Earthquake Engineering (NCREE) in Taiwan. The geometries and details (Figure 2) were selected to be representative of elements used in an eight-story frame building. Final dimensions and reinforcement details of the frames were influenced by the following considerations: laboratory and shaking table limitations, replication of column details used in existing buildings, desired failure mode, and cost. The target failure mode is intended to be damage leading to collapse that would enable examination of gravity load redistribution during the test. The column details and loading were chosen to be typical of 1960s and 1970s hospital building construction, with widely spaced ties formed with 90 degree hooks. The ratio of beam stiffness to column stiffness was considered to be similar to existing buildings. Since the overall width of the frame, and consequently the beam length, were limited by the dimensions of the shaking table; the beam depth was adjusted to achieve the target beam-to-column stiffness ratio. Beam transverse reinforcement with closed stirrups and 135° hooks provide sufficient shear strength to develop full flexural strength, while longitudinal reinforcement was chosen to create a weak-column-strong-beam mechanism typical of the older concrete construction. Neither beams nor columns have lap splices to eliminate the splicing effects from the scope of this study. Slabs are cast with the beams to include the effect of slabs on the beam stiffness and the joint demands.

Beam-column joints in non-seismically detailed concrete frames are frequently constructed without transverse reinforcement and are vulnerable to shear and axial failure during strong ground shaking. However, to separate the collapse behavior due to column failure from that resulting due to joint failure, specimens MCFS and HCFS incorporate well-confined joints and failure of the columns is expected to precipitate collapse of the frame. In contrast, MUF provides sufficient confinement in the columns to ensure a flexural response, while eliminating the confinement from the first floor joints leads to a collapse mode which is expected to be dominated by joint failure. Constructing MUFS with no confinement in the first-floor joints and light transverse reinforcement in the columns provides the opportunity to study the sequence of failure in a typical existing building frame. Discontinuity of the columns above the second floor makes the joints, particularly the exterior joints, susceptible to early failure; therefore, joints at second level are confined for all specimens.

Columns of all specimens except MUF have wide spacing of transverse reinforcement making them vulnerable to shear failure, and subsequent axial load failure, during testing. As one of the columns fails, shear and axial load will be redistributed to the other columns. The test specimens are constructed vertically similar to real structural frames. Reinforcement cages are assembled and instrumented with strain gages. Approximately 60 strain gages will be located on longitudinal and transverse reinforcement throughout the frame specimens.

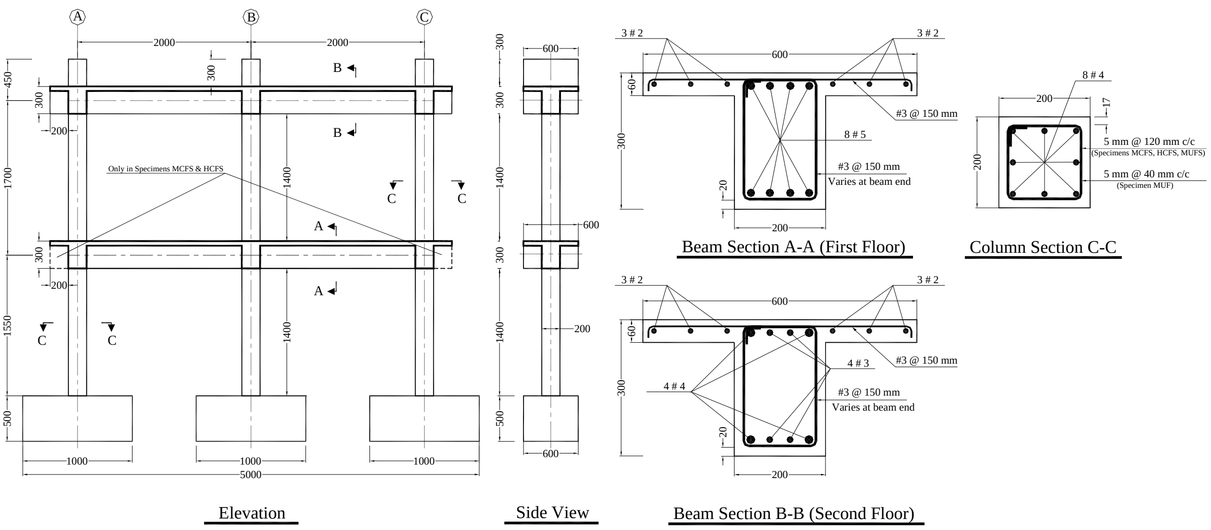

Figure 2. Shaking table test specimen and reinforcement details

The specimen design began with the size selection for the columns and beams. Given the complexity of desired test frame behavior and failure mechanisms, a detailed analytical model, rather than classical design methods, was used to design the test frame. An extensive parametric study was performed to determine optimal test frame final dimensions and details, considering the common full-scale columns in existing buildings. Columns with 200 mm×200 mm square section and eight deformed #4 bars for longitudinal reinforcement were selected (longitudinal reinforcement ratio = 0.026). Column transverse reinforcement was selected as 5mm hoops at 120 mm for specimens with flexure-shear-critical columns (MCFS, HCFS, and MUFS), while the spacing was reduced to 40 mm for MUF with ductile columns. The resulting transverse reinforcement ratio for the flexure-shear-critical and flexure-critical columns was ρ''=0.16% and 0.49%, respectively ($\rho''=A_{st}/bs$ where, A_{st} is the area of transverse reinforcement with spacing s, and b is the column width). Using ASCE/SEI 41 (2008), the ratio of the plastic shear demand on the columns (V_p) to the nominal shear strength (V_n) was estimated to be 0.84 for the flexure-shear-critical columns, which complies with the ASCE/SEI 41 (2008) definition of flexural-shear-critical columns. V_p/V_n for the columns from the MUF specimen is 0.41, consistent with the definition of flexure-critical columns. Material properties will be tested and recorded during construction; however, in order to predict the behavior of the structural elements in this paper, the properties recorded in previous tests at NCREE were employed. The compressive strength of concrete was considered to be 28 MPa, while the yield strength of the longitudinal bars in the columns was taken as 482 MPa. The stress-strain model developed by Mander et al. (1998) was used to determine the constitutive relationship for confined and unconfined concrete for the columns.

Based on Figure 2, and for ease of reference throughout this paper, columns of the test frame will be referred to using the following nomenclature. Columns will be referred to by their axis letter (see Figure 2) and story number; thus Column A1 is the first-story column at axis A. Joints will follow a similar nomenclature with the number indicating the floor number they are on; thus Joint A1 is the joint above Column A1.

3.2. Loading and Test Setup

The specimens will be constructed vertically in an area outside the NCREE facility and moved onto the shaking table where it will be bolted to six load cells (two per column), which are previously bolted to the shaking table. A stiff steel frame, bolted to the table, is used to brace the specimens in the out-of-plane direction by means of frictionless rollers at each beam level which allow free in-plane motion (both horizontal and vertical) of the frame. Rigid transverse steel beams are connected to the supporting frame to catch the specimen after collapse and prevent any damage to the shaking table.

Subsidiary masses are added to the specimens in the form of lead weights attached to the beams. Loads are distributed equally to all beams, approximately uniformly distributed along beam spans. This layout will simulate the loading effects of one-way slabs framing into the beams. The structure was intended to represent a hospital building with higher dead and live load demand than regular residential buildings. Considering the frame as half-scale, and scaling the loading suggested by the Taiwanese Building Code for such occupancy, each beam will carry a total weight of 10 kN. Each frame was assumed to be part of an eight-story building and element sizes were selected accordingly; however, only first two stories of the frame are constructed due to cost constrains and to maximize the scale of the specimen. To account for the inertial forces from the upper stories, lead packets with a weight of 60 kN on each beam will be connected to the frame such that only lateral forces are transmitted to the specimens. The inertial mass will be supported on rollers mounted on supporting frames on either side of the specimen (Figure 3, section A-A). The connection mechanism between the inertial mass and the specimen (Figure 3, section B-B) was designed such that the inertia force can be transferred to the specimen while the vertical deformation of the columns is not restrained.

The column axial loads from the upper stories will be achieved by prestressing the columns to the shaking table using pressure-controlled hydraulic jacks. A transverse steel girder (Figure 3, section B-B), placed on a pin at the top of each column, transfers the axial load to the columns. A clevis pin, aligned with the intended direction of shaking, is installed on each end of the girder. A high-strength threaded rod attaches the clevis pin to the hydraulic jack which is secured to the shaking table with another clevis pin. A pressure-regulating valve will ensure the applied axial load will be approximately constant during the test. Note that this method of axial load application does not correctly account for P-delta effects; however, collapse of the frames is expected to be controlled by material degradation (shear and axial failure) rather than P-delta instability. In order to observe the effects of axial load on behavior of non-ductile columns, the middle column of Specimens MCFS, MUFS, and MUF will be subjected to a moderate axial load ($0.2f'_cA_g$). The middle column of Specimen HCFS will be prestressed to an axial load of $0.35P_0$ which is used by Chapter 21 of ACI 318 to distinguish gravity columns requiring seismic detailing similar to columns of the lateral force resisting system (ACI 318 2008). The exterior columns of all frames will carry half of the axial loads applied to their corresponding middle columns. Axial load failure is expected to be more gradual for the columns with low axial load and more sudden for the columns with high axial load.

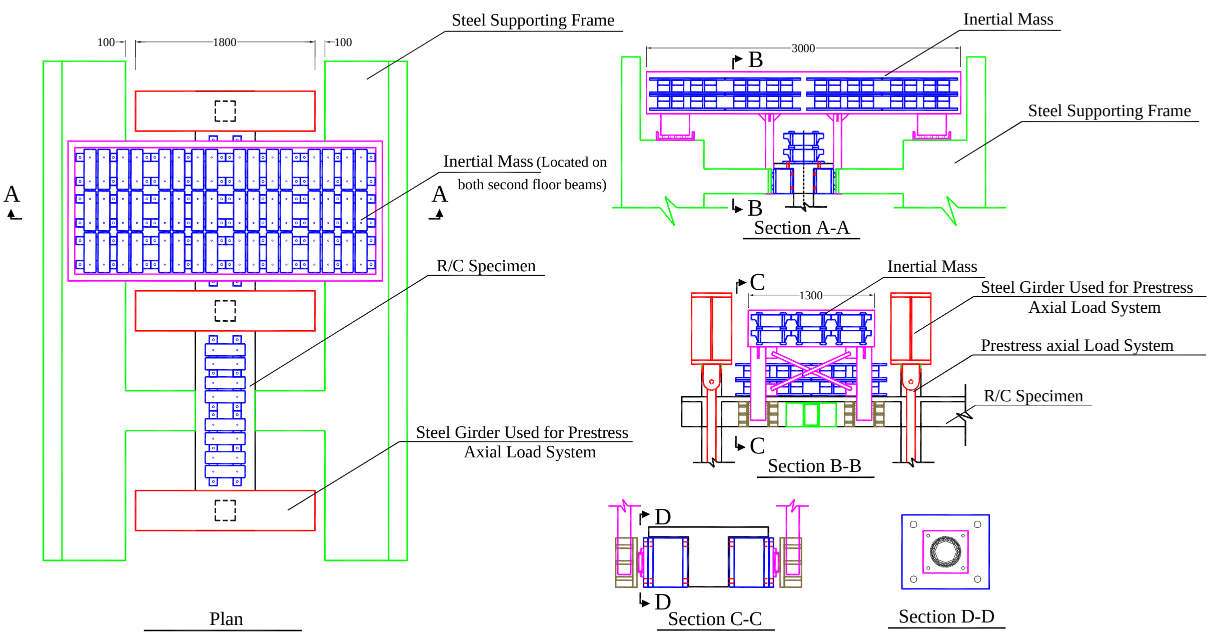

Figure 3. Prestressing and Inertial mass system

Specimen instrumentation will consist of: 1) force transducers (or load cells) that measured shear, axial load, and bending moments at the base of the frame footings; 2) strain gages on longitudinal and transverse reinforcement in columns, beams, and joints; 3) accelerometers for horizontal and vertical accelerations of both beams; and 4) displacement transducers to measure both local column and global frame deformations.

4. ANALYSIS

4.1. Analytical Models

Elwood (2004) describes analytical models that allow for simulation of the shear and axial behavior of flexure-shear-critical columns up to and including collapse of a building frame system. These models were defined and implemented as LimitState material models in OpenSEES (2008) and will be used throughout the analysis phase of this project. The implementation of shear and axial failure models is done through the addition of zero-length spring elements with the LimitState model properties at the end of column elements. The backbone response of the spring element is modified when the drift demand on the column exceeds the shear and axial drift capacity models shown in Equations 4.1 and 4.2, respectively.

$$\frac{\Delta_s}{L} = \frac{3}{100} + 4\rho'' - \frac{1}{40}\frac{\upsilon}{\sqrt{f'_c}} - \frac{1}{40}\frac{P}{A_g f'_c} \geq \frac{1}{100} \tag{4.1}$$

$$\frac{\Delta_a}{L} = \frac{0.2}{2.1+0.5P(s/A_{st}f_{yt}d_c)} \tag{4.2}$$

where ρ'' is the column transverse reinforcement ratio, υ is the shear stress ratio, P is the axial load, A_g is the gross section area, A_{st} is the transverse reinforcement area with yield strength f_{yt} and spacing s, and d_c is the depth of the column core between centerlines of the ties. Prior to shear or axial failure, the corresponding spring is linear-elastic with the equivalent elastic stiffness of the column in the direction of the spring. Once the column element experiences the drift limit defined by Equations 4.1 or 4.2, the related spring backbone curve is modified to a degrading response. Further details of the column failure models can be found in Elwood (2004). It should be noted that the axial-drift model (Equation 4.2) is based on a relatively small number of reversed-cyclic column tests and results of the dynamic tests proposed here will be employed to verify and refine the model.

For the sake of brevity, only the blind prediction of the behavior of Specimens MCFS and HCFS is presented here. Figure 4 shows a schematic of the model for these two specimens. Each column consisted of a single force-based nonlinear beam-column element with 5 integration points and two zero-length elements located at the top and bottom of the beam-column element. Each of the zero-length elements is defined by two nodes at the same location. The nodes are connected by multiple material objects to represent the force-deformation relationship for the element. The top zero-length elements for the columns include shear and axial springs whose behavior is defined by LimitState material models described in section 4.1. To account for the flexibility due to slip of the longitudinal reinforcing bars from the beam and footing, elastic rotational slip springs were included in zero-length elements at both ends of each of the column elements. The rotational stiffness recommended by Elwood and Eberhard (2008) is used for the slip springs (Equation 4.3).

$$K_{slip} = \frac{8u}{d_b f_s} EI_{flex} \tag{4.3}$$

where, u is the bond stress (assumed to be $0.8\sqrt{f_c'} = 4.2$ MPa), d_b is the nominal diameter of the longitudinal reinforcement, f_s is the tensile stress in the longitudinal reinforcement, and EI_{flex} is effective flexural stiffness obtained from a moment-curvature analysis.

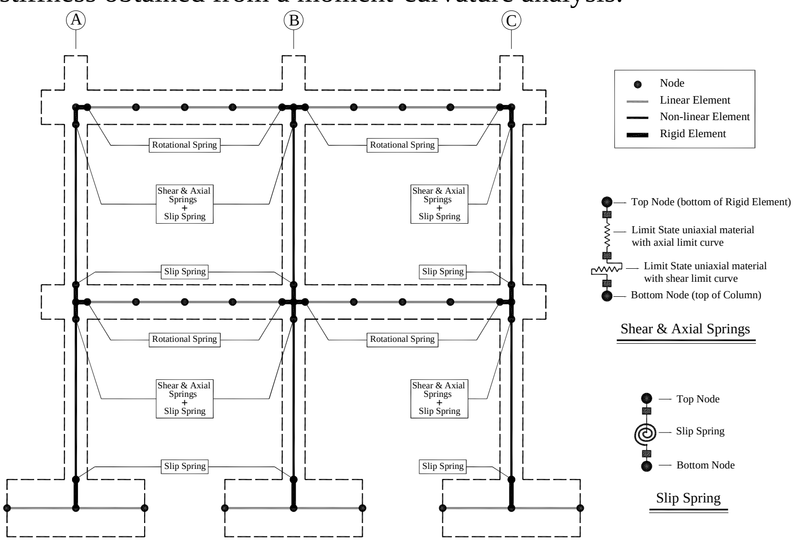

Figure 4. Model of shaking table Specimens MCFS and HCFS

The beams were not expected to exhibit a significant degree of nonlinearity during testing; therefore, for computational efficiency, they were modeled as elastic with lumped plasticity rotation springs at the face of the joints. The equivalent flexural stiffness was derived from moment-curvature analysis, which produced a flexural stiffness parameter, $EI_{flex} = 0.4EI_{gross}$, where E is the concrete modulus of elasticity and I_{gross} is the gross section moment of inertia. Joints in Specimens MCFS and HCFS are well-confined by transverse reinforcement and therefore, the results presented here were obtained using a rigid joint model.

The equivalent viscous damping was chosen as 2% of critical for the fundamental mode of the frame (0.33 seconds) using mass-proportional damping. Note that stiffness-proportional damping could not be used in this model. At shear and axial failure, the stiffness of the zero-length springs changes very suddenly which causes a large increase in velocity. This induces unrealistically large damping forces at the node connecting the springs to the beam-column element if stiffness-proportional damping is used (Elwood and Moehle 2003). No mass was modeled at this node, and hence, the mass-proportional damping matrix contains zeros for degrees of freedom at this node; thus, the increase in velocity does not generate unrealistic damping forces when mass-proportional damping is used.

To validate the model and get a sense of the damage sequence of the frame up to collapse, the analytical model was subjected to a nonlinear static (pushover) analysis with an inverted-triangular load distribution; however, the results of this study are omitted due to space limitations.

4.2. Test Frame Simulation

The input motion for the tests is yet to be selected, but the EW component of the TCU082 accelerogram from the 1999 Chi-Chi Taiwan earthquake was employed for the prediction presented below. The station was located in central Taiwan, and was close to typical buildings studied herein. The input motion was scaled to achieve a peak ground acceleration of 1.85g.

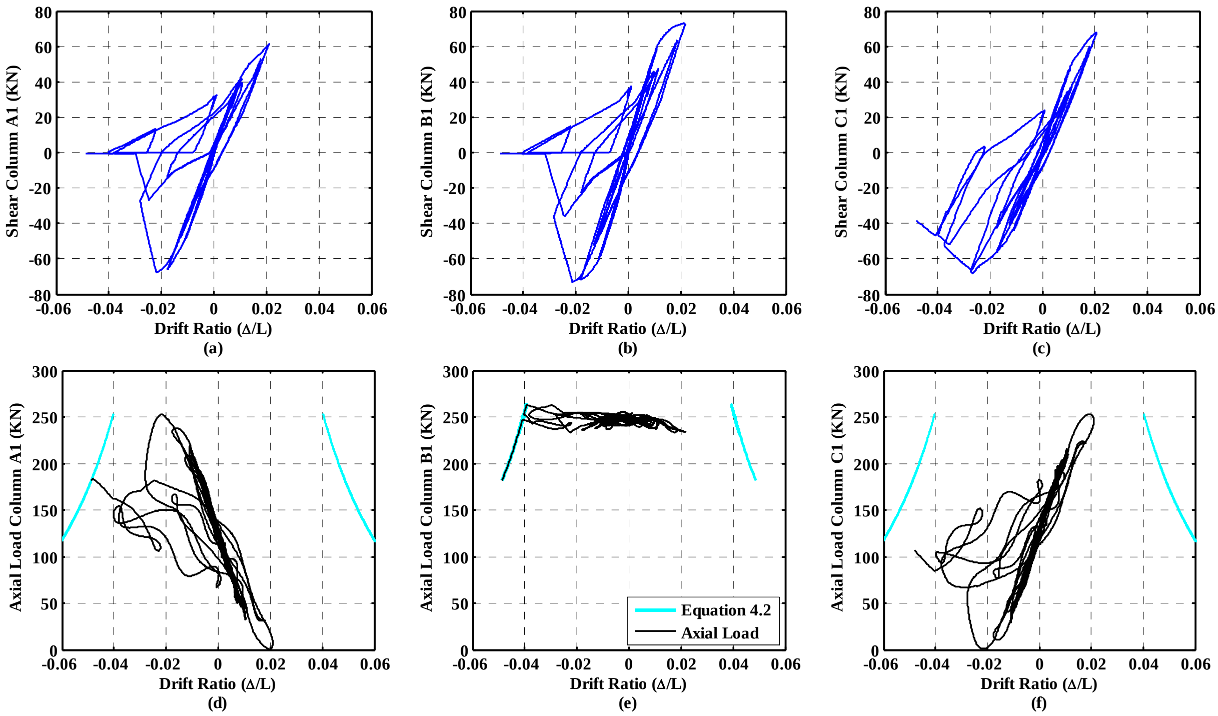

Figure 5. Shear and axial behavior of first floor of Specimen MCFS

Dimensions and detailing of the test Specimen MCFS are likely to result in concentrated damage in the columns in the first story, with relatively less damage in upper-story columns prior to collapse. Results of nonlinear dynamic analysis for shear and axial behavior of the first floor columns, under moderate axial load ($0.2f_c'A_g$), are shown in Figure 5. The predicted sequence of failures prior to collapse is as follows: the shear failure of columns B1, A1, C1, and limited failure of column B2, followed by axial failure of columns B1 and A1. Yielding of longitudinal steel of first-story columns occurs at first-story horizontal drifts between 1.0% and 1.4%, depending on the axial load. At about 2.2% horizontal drift, shear failures initiate in columns B1 and A1. Between 2.2% and 3.2% horizontal drift, a gradual loss of shear resistance is observed in columns B1 and A1. Axial failure of column B1 is initiated at 4.0% drift, followed by axial failure of column A1 at 4.9% drift. Analysis is terminated after failure of column A1 due to instability of the frame resulting in a lack of convergence in the analysis. In the analysis, axial failure of the columns occurs shortly after full degradation of the shear resistance. Data from the shaking table tests will be used to assess if this observation, commonly made based on single column tests, can be applied to frame systems. Results of analysis for Specimen HCFS, with identical details but high axial load ($0.35P_0$), suggest that the columns in the second floor may experience shear failure before the first floor columns. Axial failure is predicted for column B2 followed by axial failure of column A2.

5. SUMMARY AND CONCLUSIONS

Four reinforced concrete frames were designed to be tested at the National Center for Research on Earthquake Engineering (NCREE) in fall 2008. Results of testing the specimens are expected to shed light on the effects of high axial load on lateral and axial behavior of flexure-shear-critical columns, the behavior of unconfined joints, and the overall behavior of nonductile concrete frames up to the point of collapse. Details of the specimens and setup of the tests were described in this paper. Preliminary results of the analyses for the specimen under moderate axial load with non-ductile columns and confined joints suggest that collapse of the frame will be initiated by failure of the columns in first story, starting with the middle column. Upper floor columns will not experience shear failure. When the axial load is increased, second floor columns are more vulnerable to failure. Further investigation is required to confirm these observations for different ground motions. Comparison of the results from the analyses with the result from the shaking table tests will reveal the accuracy of the existing analytical models leading to refinement of the models and more accurate prediction of the behavior of flexure-shear-critical frames in future earthquakes.

6. ACKNOWLEDGMENTS

The study discussed above was part of a tri-national collaborative research effort on the collapse of concrete frames funded in part by the Natural Science and Engineering Research Council of Canada, the National Science Foundation (US) and the National Science Council of Taiwan. This funding is gratefully acknowledged. All opinions expressed in this paper are solely those of the authors and do not necessarily represent the views of the sponsors.

REFERENCES:

American Concrete Institute (ACI) (2008). Building Code Requirements for Structural Concrete, *ACI 318-08*, Farmington Hills, USA.

American Society of Civil Engineers (ASCE) (2008). Seismic Rehabilitation of Existing Buildings, *ASCE/SEI 41 Supplement 1*; American Society of Civil Engineers, Reston, Virginia.

Elwood, K.J. (2004). Modeling Failures in Existing Reinforced Concrete Columns, *Canadian Journal of Civil Engineering* **31:5**, 846-859.

Elwood, K.J. and Eberhard, M. (2008). Effective Stiffness of Reinforced Concrete Columns. *American Concrete Institute*; submitted for publication.

Elwood, K.J. and Moehle, J.P. (2003). Shake Table Tests and Analytical Studies on the Gravity Load Collapse of Reinforced Concrete Frames. *PEER report 2003/01*. Berkeley, Calif.: Pacific Earthquake Engineering Research Center, University of California.

Mander J.B, Priestley M.J.N, and Park R. (1998). Theoretical Stress-Strain Model for Confined Concrete. *Journal of Structural Engineering* **114:8,** 1804-1826.

OpenSEES (2008). Open System for Earthquake Engineering Simulation. Pacific Earthquake Engineering Research Centre, University of California. http://www.opensees.berkeley.edu.

Otani, S. (1999). RC Building Damage Statistics and SDF Response with Design Seismic Forces. *Earthquake Spectra* **15:3**, 485-501.